The yeast protein Ubx4p contributes to mitochondrial respiration and lithium–galactose–mediated activation of the unfolded protein response

Received for publication, October 9, 2019, and in revised form, January 22, 2020 Published, Papers in Press, January 29, 2020, DOI 10.1074/jbc.RA119.011271

Evandro A. De-Souza[‡1], Felipe S. A. Pimentel[‡1], Ana Luiza F. V. De-Queiroz[‡], Henrique Camara[§], Mikaella L. Felix-Formiga[‡], Caio M. Machado[‡], Silas Pinto[§], Antonio Galina[¶], Marcelo A. Mori[§], Monica Montero-Lomeli[‡], and Claudio A. Masuda[‡2]

From the [‡]Programa de Biologia Molecular e Biotecnologia and the [¶]Programa de Bioquímica e Biofísica Celular, Instituto de Bioquímica Médica Leopoldo de Meis, Universidade Federal do Rio de Janeiro, Rio de Janeiro 21941-902, Brazil and the [§]Department of Biochemistry and Tissue Biology, Instituto de Biologia, Universidade Estadual de Campinas, Campinas SP, 13083-970, Brazil

Edited by Ursula Jakob

In the presence of galactose, lithium ions activate the unfolded protein response (UPR) by inhibiting phosphoglucomutase activity and causing the accumulation of galactose-related metabolites, including galactose-1-phosphate. These metabolites also accumulate in humans who have the disease classic galactosemia. Here, we demonstrate that *Saccharomyces cerevisiae* yeast strains harboring a deletion of *UBX4*, a gene encoding a partner of Cdc48p in the endoplasmic reticulum–associated degradation (ERAD) pathway, exhibit delayed UPR activation after lithium and galactose exposure because the deletion decreases galactose-1-phosphate levels. The delay in UPR activation did not occur in yeast strains in which key ERAD or proteasomal pathway genes had been disrupted, indicating that the *ubx4*Δ phenotype is ERAD-independent. We also observed that the *ubx4*Δ strain displays decreased oxygen consumption. The inhibition of mitochondrial respiration was sufficient to diminish galactose-1-phosphate levels and, consequently, affects UPR activation. Finally, we show that the deletion of the AMP-activated protein kinase ortholog–encoding gene *SNF1* can restore the oxygen consumption rate in *ubx4*Δ strain, thereby reestablishing galactose metabolism, UPR activation, and cellular adaption to lithium–galactose challenge. Our results indicate a role for Ubx4p in yeast mitochondrial function and highlight that mitochondrial and endoplasmic reticulum functions are intertwined through galactose metabolism. These findings also shed new light on the mechanisms of lithium action and on the pathophysiology of galactosemia.

Lithium is one of the most common drugs used in the treatment of bipolar disorder patients. The molecular mechanisms of lithium action are not fully elucidated, but evidence points to a role for lithium as a GSK-3β inhibitor, as an inducer of inositol depletion, among others hypotheses (1). Lithium is also capable of inhibiting the activity of the enzyme phosphoglucomutase because it competes with its cofactor magnesium (2). Because of this inhibition, cells treated with lithium in the presence of galactose accumulate toxic metabolites of the Leloir pathway in yeast (2–4) and human cells (5). Accumulation of intermediate metabolites of galactose metabolism such as galactose-1-phosphate also occurs in patients with classic galactosemia, an inborn error of metabolism caused by mutations in the *GALT* gene (6, 7). Yeast is a eukaryotic cell model commonly employed in studies to better understand human diseases because of its similarities with human metabolism and its vast toolkit for genetic manipulation (8). Yeast cells treated with lithium in the presence of galactose exhibit modifications in cellular homeostasis such as changes in glycogen, calcium, and phosphate levels and a metabolic shift from fermentation to respiration (3, 9–11). Another important feature of lithium/galactose treatment is the increase in endoplasmic reticulum (ER)[3] stress and unfolded protein response (UPR), both in yeast and in human cells (3, 5). This UPR activation depends on the synthesis of galactose-1-phosphate and also occurs in genetic models of classic galactosemia (3, 12, 13).

The ER is an organelle in which protein folding, glycosylation, and lipid synthesis take place. In yeast, during ER stress conditions, the communication between ER and nucleus is mediated by the conserved kinase/endoribonuclease protein Ire1p. This transmembrane protein, together with the tRNA ligase Trl1p, promotes the cytosolic splicing of the *HAC1*

This work was supported by research grants from Conselho Nacional de Desenvolvimento Científico e Tecnológico, and Coordenação de Aperfeiçoamento de Pessoal de Nível Superior; by Fundação Carlos Chagas Filho de Amparo a Pesquisa do Estado do Rio de Janeiro Grants E-26/203.203/2015 (to M. M.-L.) and E-26/010.000837/2016 (to C. A. M.); and by Fundação de Amparo à Pesquisa do Estado de São Paulo Grant 2017/01184-9 (to M. A. M.). This work was also supported in part by Conselho Nacional de Desenvolvimento Científico e Tecnológico fellowships (to E. A. D.-S., F. S. A. P., A. L. F. V. D.-Q., C. M. M., and M. L. F.-F.), Fundação Carlos Chagas Filho de Amparo a Pesquisa do Estado do Rio de Janeiro fellowship E-26/200.790/2019 (to E. A. D.-S.), and Fundação de Amparo à Pesquisa do Estado de São Paulo fellowships 17/04377-2 (to S. P.) and 17/01339-2 (to H. C.). The authors declare that they have no conflicts of interest with the contents of this article.

This article contains Figs. S1–S6.

[1] These authors contributed equally to this work.

[2] To whom correspondence should be addressed. Tel.: 55-21-25618226; Fax: 55-21-22708647; E-mail: cmasuda@bioqmed.ufrj.br.

[3] The abbreviations used are: ER, endoplasmic reticulum; UPR, unfolded protein response; ERAD, ER-associated degradation; AMPK, AMP-activated protein kinase; UBX, ubiquitin regulatory X; ANOVA, analysis of variance.

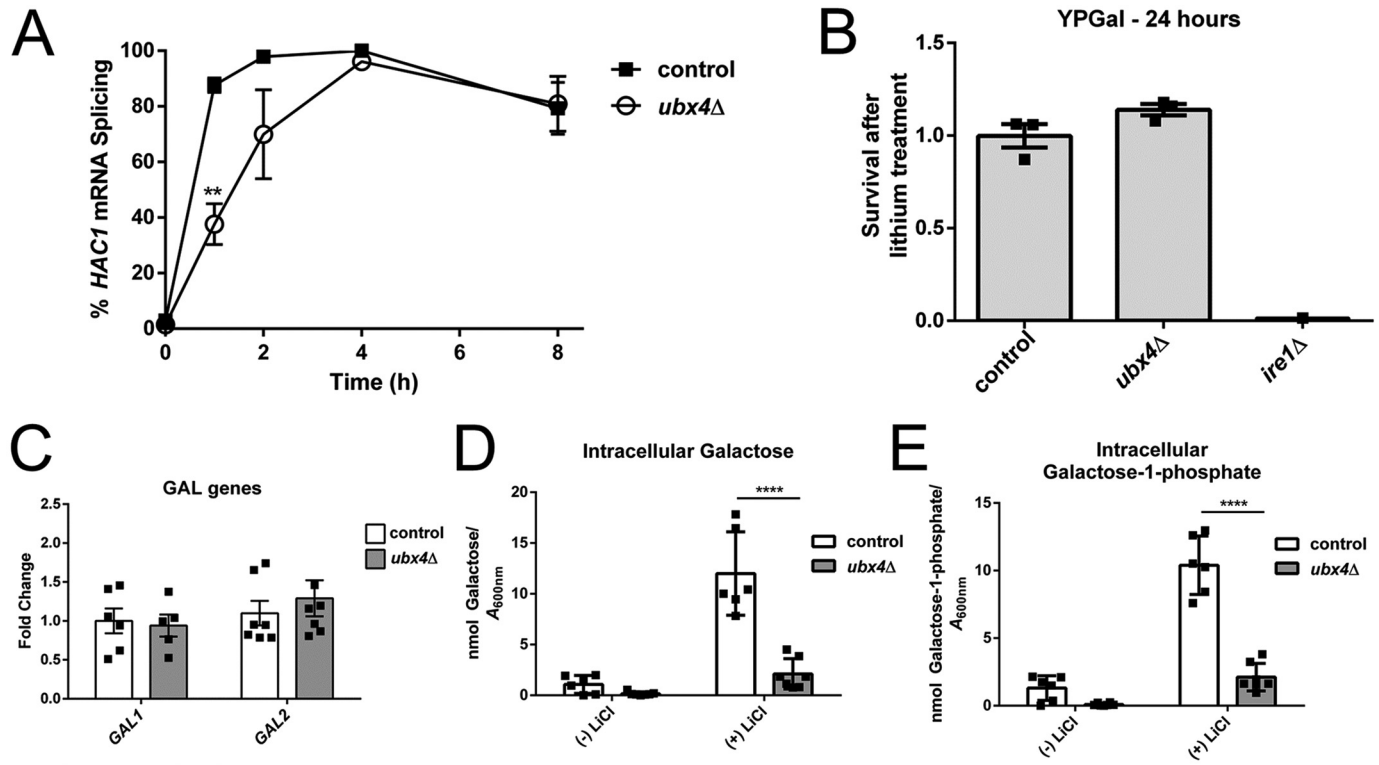

Figure 1. *UBX4* is necessary for proper UPR activation and galactose metabolism in lithium–galactose–treated cells. *A*, the levels of *HAC1* mRNA splicing were monitored at the indicated time points by RT-PCR in control and *ubx4*Δ cells grown in YPGal and treated with 30 mM LiCl. The data are presented as means ± S.E. Two-way ANOVA was performed with Sidak's multiple comparisons test. **, $p < 0.01$. *B*, the indicated strains, control ($n = 3$), *ubx4*Δ ($n = 3$), and *ire1*Δ ($n = 1$) were grown in the presence of 30 mM LiCl for 24 h in YPGal and, after this incubation period, plated on YPD for colony-forming unit measurement. Normalization was performed by the number of colony-forming units in strains grown in YPGal without LiCl. *C*, relative expression levels of *GAL1* and *GAL2* mRNAs, normalized by *TFC1* gene, were determined by quantitative RT-PCR from control or *ubx4*Δ cells grown in YPGal ($n = 5$–7 biological replicates). Student's *t* test was used at this analysis to compare the control *versus ubx4*Δ groups, and no statistically significant difference between groups was observed. We obtained similar results by normalizing the data with *TAF10* gene (data not shown). *D* and *E*, levels of intracellular galactose (*D*) or intracellular galactose-1-phosphate (*E*) were measured on the indicated strains grown in YPGal for 1 h in the presence or absence of 30 mM LiCl ($n = 6$–7 biological replicates). ****, $p < 0.0001$. $A_{600\ nm}$, absorbance at 600 nm.

mRNA, which in turn codes for the transcription factor Hac1p (14, 15). Hac1p induces the activation of genes responsible for restoring ER homeostasis such as ER-resident chaperones (16). The Ire1/Hac1 branch of UPR is the only one present in yeast and is conserved from yeast to mammals (Ire1α/Xbp1), being relevant to different diseases (17–20). A second way that cells can cope with ER stress is by alleviating proteotoxicity through the ER-associated protein degradation (ERAD) pathway. ER-localized misfolded proteins retrotranslocate to the cytosol, where they are ubiquitinated and degraded by the proteasome (21). In this work, we demonstrate the function of Ubx4p (Cui1p), a Cdc48p protein adaptor in the ERAD pathway (22, 23), on the cellular adaption to lithium and galactose toxicity. Ubx4p contains a ubiquitin regulatory X (UBX) domain that mediates physical interaction with Cdc48p (24) and an ubiquitin-like domain that is commonly found in proteins that can interact and recruit proteasome (25). In fact, both UBX and ubiquitin-like domains are necessary for Ubx4p interaction with the proteasome (23). Ubx4p homolog in humans is called ASPL/TUG, a protein that interacts with p97/VCP (homolog of Cdc48 in mammals) (26). Importantly, the expression of *ASPL/TUG* in an *ubx4*Δ strain is capable of recovering the proteasome localization defect of this strain. ASPL/TUG in mammals can also bind to the GLUT4 (glucose transporter type 4) and control its translocation to the plasma membrane upon insulin stimulation (27–29).

Here we show a novel and ERAD-independent role for Ubx4p in controlling mitochondrial and galactose metabolism. Our data demonstrate that *UBX4* deletion impairs mitochondrial respiration, which in turn affects galactose metabolism and activation of the UPR. For these reasons, *ubx4*Δ mutants are less tolerant to lithium/galactose.

Results

Based on a genetic screen to identify new regulators of UPR activation induced by lithium and galactose treatment, we identified that the deletion of the *UBX4*/*YMR067C* gene delays UPR activation (Fig. 1*A*). In this context, the inhibition of the UPR pathway (*e.g.* deletion of *IRE1* or *HAC1* genes) causes loss of cell viability (3). We did not observe the same for the *ubx4*Δ mutant, which remained viable after 24 h of treatment with lithium in the presence of galactose (Fig. 1*B*), probably because this strain can still fully activate UPR (as measured by *HAC1* mRNA splicing) after 4 h of treatment. These results suggest that Ubx4p is not interfering directly with Ire1p activity. Accordingly, the deletion of *UBX4* did not affect UPR activation by tunicamycin treatment (Fig. S1).

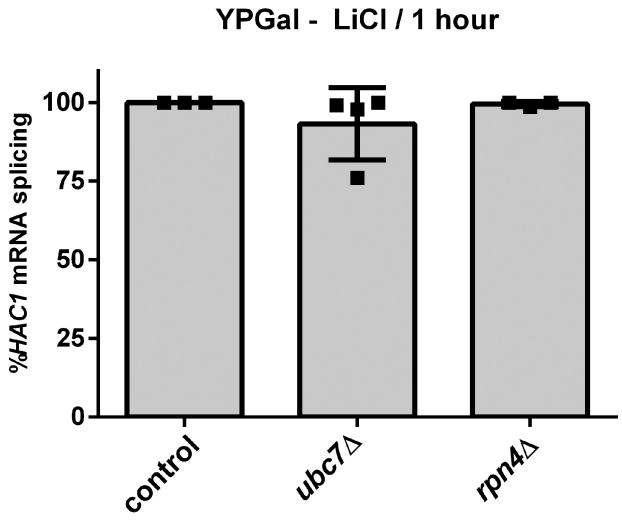

Figure 2. *UBX4*, but not ERAD/proteasome, regulates *HAC1* mRNA splicing in lithium/galactose-treated cells. The levels of *HAC1* mRNA splicing were monitored by RT-PCR in control, *ubc7*Δ, and *rpn4*Δ strains grown in YPGal and treated with 30 mM LiCl for 1 h (n = 3–4 biological replicates). One-way ANOVA with Dunnett's multiple comparison test was performed, and we did not observe any statistically significant difference between the groups.

This raised the hypothesis that the deletion of *UBX4* is delaying ER stress occurrence in a lithium–galactose–specific manner. As previously described by our group, UPR activation in models of galactosemia can be prevented by the deletion of yeast galactokinase *GAL1* (3), suggesting that the synthesis of galactose-1-phosphate is an essential event for the UPR activation in this condition. Although we did not observe differences in the expression of genes of Leloir pathway (*GAL1* and *GAL2*) (Fig. 1*C*), we measured the galactose and galactose-1-phosphate levels in the *ubx4*Δ mutant, and we observed an 82–85% decrease in galactose (Fig. 1*D*) and a 77–93% decrease in galactose-1-phosphate levels (Fig. 1*E*) when compared with a control strain, even without lithium. These results suggest that the delayed UPR activation in the *ubx4*Δ strain is due to the overall decreased levels of galactose-1-phosphate accumulated in this strain.

Ubx4p is known to participate in the ERAD pathway and to regulate proper proteasome localization (22, 23). Thus, we reasoned that mutations in other components of these pathways would also influence UPR activation in lithium/galactose-treated cells. Nonetheless, the deletion of *UBC7*, a central effector of ERAD pathway (21, 30), or the deletion of *RPN4*, a transcription factor and master regulator of proteasome genes (31–33), did not affect the capacity of the cell to induce *HAC1* mRNA splicing when treated with lithium and galactose (Fig. 2).

A strategy to reduce lithium–galactose toxicity is to prevent galactose-1-phosphate accumulation (3, 4, 34). We assumed that because the deletion of *UBX4* decreases intracellular galactose-1-phosphate content, the *ubx4*Δ would be more tolerant to the treatment of lithium and galactose. Surprisingly, we observed that *UBX4* deletion results in a decreased cellular tolerance to lithium in galactose-containing medium but not in glucose-containing medium (Fig. 3*A*). A decrease of ERAD or proteasome cellular function does not explain this increased sensitivity because neither the deletion of *RPN4* nor the deletion of *UBC7* modified the cellular sensitivity to lithium and galactose (Fig. 3*B*). We also tested mutations in other components of these pathways but could not observe significant differences in cell growth among those strains (Fig. S2).

Our data suggested that the deletion of *UBX4* might be acting on the lithium–galactose tolerance via other mechanism rather than regulating galactose metabolism. Previous work suggested that the deletion of the *UBX4* gene increases the frequency of *petite* colonies, which in general is related to deficiencies in mitochondrial metabolism (35). Hence, we monitored the respiration capacity of this strain, and we observed a greater than 10-fold decrease in oxygen consumption rate in the *ubx4*Δ cells compared with the cells of a control strain when grown in galactose (Fig. 4*A*). The impaired galactose metabolism observed in *ubx4*Δ does not seem to be solely responsible for the decreased mitochondrial respiration because the *gal1*Δ strain, which cannot metabolize galactose because of the lack of galactokinase, presents only a slight decrease in mitochondrial oxygen consumption under the same conditions. This result is expected because these strains are growing in a rich medium containing other carbon sources, such as amino acids, which can sustain mitochondrial respiration when galactose metabolism is impaired. We also observed that the deletion of *UBX4* reduced oxygen consumption in the absence of galactose metabolism, for example, when cells were grown on YPGly (medium containing glycerol, a nonfermentable carbon source) (Fig. S3*A*). The deletion of neither *UBC7* nor *RPN4* affected oxygen consumption rates (Fig. 4*A* and Fig. S3*A*), suggesting that an impairment of ERAD or proteasome function does not contribute for this *ubx4*Δ phenotype. The fact that mitochondrial preparations from *ubx4*Δ cells present decreased oxygen consumption capacity when compared with mitochondrial preparations from a control yeast strain (Fig. S3, *B* and *C*) further supports the hypothesis that the effect of *UBX4* deletion on oxygen consumption *in vivo* is not only due to its impact on galactose metabolism.

A hypothesis to explain the decreased tolerance to lithium and galactose observed in the *ubx4*Δ strain is that, under this condition, cells are more dependent on respiration, and because the *ubx4*Δ strain presents a decreased mitochondrial oxygen consumption rate, it cannot grow properly. This is in line with previous data from our group showing that lithium–galactose–treated control cells have a metabolic shift from fermentation to respiration (11). Accordingly, if we simulate the *ubx4*Δ defects in both galactose and mitochondrial metabolism by growing the *gal1*Δ strain in the presence of antimycin A, an inhibitor of mitochondrial complex III, the cells become unable to grow on galactose (Fig. 4*B*).

We reasoned that mitochondrial function could be upstream of galactose metabolism and UPR activation in lithium-treated yeast cells. Accordingly, previous studies showed that *GAL1* gene expression is down-regulated in strains with mutations in components of the mitochondrial electron transport chain or in yeast strains with reduced mitochondrial membrane potential (36, 37). On the other hand, another study observed that yeast cells depleted of mitochondrial DNA (rho^0) present an increase in Gal4-dependent transcription (38). Nevertheless, it

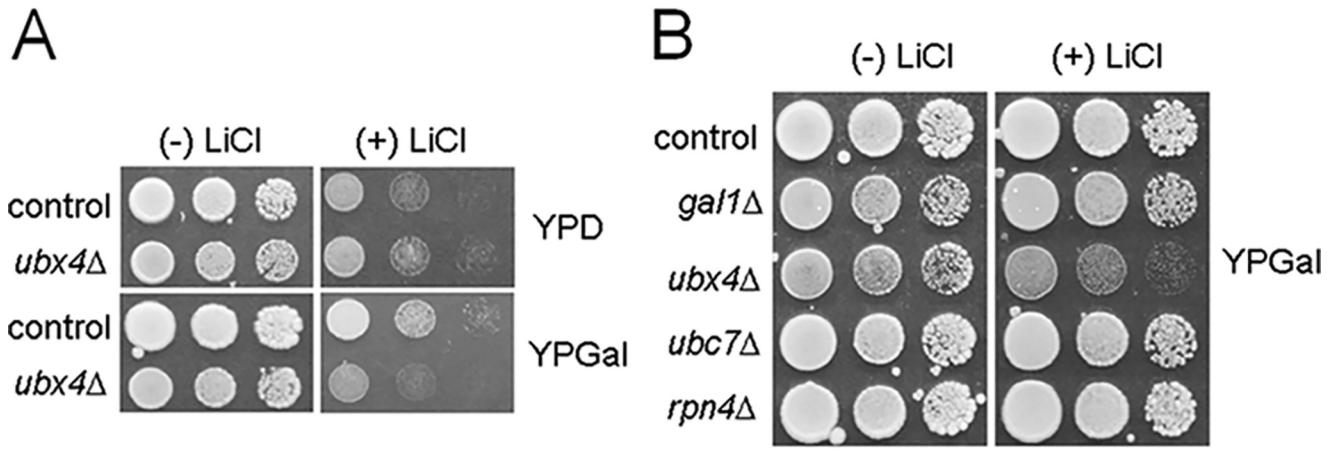

Figure 3. *UBX4* is necessary for the cellular adaption to lithium and galactose treatment. *A*, the indicated strains were grown in glucose (YPD) or galactose (YPGal) containing media. The LiCl concentration added in YPD and YPGal plates were 300 and 10 mM, respectively. The plates were incubated at 30 °C for 3 days. *B*, the indicated strains were grown in YPGal in the presence or absence of 10 mM LiCl for 3 days. Representative results of three independent experiments are shown.

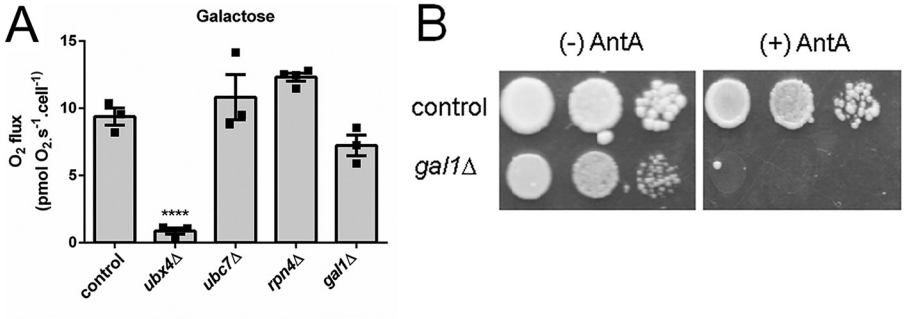

Figure 4. Mitochondrial respiration is diminished on *ubx4*Δ mutant. *A*, the oxygen consumption rate was measured in control, *ubx4*Δ, *ubc7*Δ, *rpn4*Δ, and *gal1*Δ strains grown in YPGal ($n = 3–4$ biological replicates). One-way ANOVA with Dunnett's multiple comparison test was performed using the control group for comparison. ****, $p < 0.0001$. *B*, the control and *gal1*Δ strains were grown in YPGal in the presence or absence of 0.01 μM antimycin A (*AntA*) for 3 days at 30 °C. Representative results of three independent experiments are shown.

remains to be tested whether mitochondrial dysfunction promotes alterations in galactose metabolite levels. To test these hypotheses under our growth conditions, we first inhibited yeast mitochondrial function by deleting *COQ3* or *ATP7* genes, which impairs mitochondrial respiratory chain function (39–41) (Fig. 5*A*). These mutants recapitulated all *ubx4*Δ phenotypes, including decreased cell growth on lithium and galactose (Fig. 5*A*), the decrease in galactose-1-phosphate levels ($p < 0.0001$ two-way ANOVA 30 mM of LiCl; control strain *versus atp7*Δ or *coq3*Δ) (Table 1), and the defect in *HAC1* mRNA splicing induced by lithium and galactose treatment (Fig. 5*B*).

It was previously observed that the deletion of the yeast AMPK homolog *SNF1* increases the oxygen consumption rate when yeast cells are grown in glucose medium (42). We observed a similar increase when *snf1*Δ strains were grown in the presence of galactose (Fig. 6*A*). We then deleted the *SNF1* gene in the *ubx4*Δ strain to test whether this deletion could recover *ubx4*Δ mitochondrial function. Surprisingly, *SNF1* deletion totally recovered *ubx4*Δ oxygen consumption capacity (Fig. 6*A*). Accordingly, the deletion of *SNF1* was capable of recovering the adaption capacity to lithium and galactose treatment and the UPR activation of the *ubx4*Δ strain (Fig. 6, *B* and *C*). When we measured galactose-1-phosphate levels in these mutants, we noted that the deletion of *SNF1* partially recovered galactose-1-phosphate levels in the *ubx4*Δ strain growing in YPGal (Table 1). Despite the fact that *snf1*Δ cells treated with lithium and galactose exhibited an ~40% reduction in galactose-1-phosphate levels when compared with the control strain (Table 1) ($p < 0.0001$ two-way ANOVA 30 mM of LiCl; control strain *versus snf1*Δ), the deletion of *SNF1* partially restored the levels of galactose-1-phosphate in the *ubx4*Δ strain (Table 1) ($p = 0.0677$ two-way ANOVA 30 mM of LiCl; *ubx4*Δ *versus ubx4*Δ*snf1*Δ). Galactose-1-phosphate is believed to be a toxic metabolite in the cell when accumulated, and although the *ubx4*Δ*snf1*Δ strain has higher levels of galactose-1-phosphate than the *ubx4*Δ mutant, the former grows better when treated with lithium and galactose, probably because of the increase in the oxygen consumption rate mediated by the deletion of *SNF1*.

Discussion

In this work, we showed that *UBX4* is necessary for proper UPR activation in cells treated with lithium in the presence of galactose. We presented evidences that *UBX4* does not regulate Ire1p activity directly. Instead, it diminishes ER stress by decreasing the intracellular content of galactose-1-phosphate (and possibly other Leloir pathway metabolites), accumulation of which is necessary for UPR activation in these conditions (3). Curiously, we did not observe any changes in UPR activation in

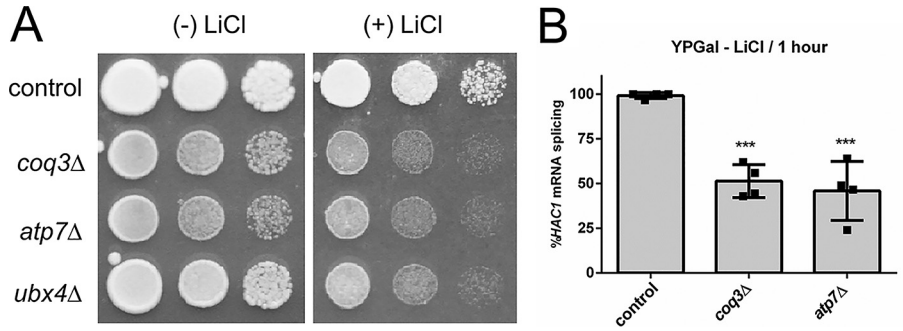

Figure 5. Mitochondrial function is necessary for proper UPR activation and cellular adaptation to lithium/galactose treatment. *A*, the indicated strains were grown in YPGal or YPGal and 30 mM LiCl for 3 days at 30 °C. Representative results of at least three independent experiments are shown. *B*, The levels of *HAC1* mRNA splicing were monitored by RT-PCR at control, *coq3*Δ, and *atp7*Δ strains grown in YPGal and treated with 30 mM LiCl for 1 h ($n = 4–5$ biological replicates). ***, $p < 0.001$; ****, $p < 0.0001$. One-way ANOVA with Dunnett's multiple comparison test was performed.

Table 1
Levels of intracellular galactose and galactose-1-phosphate

Strain	Treatment	Galactose (nmol/O.D.)	Galactose-1-phosphate (nmol/O.D.)
Control	YPGal	1.07 ± 0.87	1.31 ± 0.91
*ubx4*Δ	YPGal	0.16 ± 0.17	0.09 ± 0.09
*snf1*Δ	YPGal	1.19 ± 0.83	1.40 ± 0.92
*ubx4*Δ*snf1*Δ	YPGal	0.52 ± 0.30	0.89 ± 0.67
*coq3*Δ	YPGal	0.32 ± 0.09	0.046 ± 0.08
*atp7*Δ	YPGal	1.16 ± 0.92	0.18 ± 0.18
Control	YPGal + 30 mM LiCl (1 h)	11.99 ± 4.10	9.45 ± 1.61
*ubx4*Δ	YPGal + 30 mM LiCl (1 h)	2.11 ± 1.49	2.11 ± 1.02
*snf1*Δ	YPGal + 30 mM LiCl (1 h)	6.26 ± 1.98	6.50 ± 1.35
*ubx4*Δ*snf1*Δ	YPGal + 30 mM LiCl (1 h)	2.94 ± 1.17	3.94 ± 1.39
*coq3*Δ	YPGal + 30 mM LiCl (1 h)	4.88 ± 1.42	2.46 ± 0.20
*atp7*Δ	YPGal + 30 mM LiCl (1 h)	6.88 ± 3.82	2.5 ± 0.65

strains that are defective on ERAD or proteasome activity, suggesting that the effect of *UBX4* deletion does not relate to these previously described Ubx4p functions. Importantly, we found that *UBX4* deletion has an impact on mitochondrial oxygen consumption rates, which in turn affects galactose metabolism and consequently UPR activation in lithium–galactose–treated cells (Fig. 6*D*).

The human homolog of Ubx4p, TUG/ASPSCR1, was initially described as a GLUT4 tether, which interacts with this transporter via its conserved UBX domain, thus regulating GLUT4 membrane exposure under insulin stimulation (27). Curiously, our data show that *ubx4*Δ has reduced levels of intracellular galactose, even when compared with that of *atp7*Δ or *coq3*Δ mutants. That could be explained if yeast Ubx4p could directly regulate hexose carrier activity. It will be interesting to test this possibility in the future. This is in agreement with data showing that the galactose transporter *GAL2* mRNA level was not reduced on *ubx4*Δ strain (Fig. 1*C*), indicating that *GAL2* could be regulated at the post-transcriptional level.

To test whether *UBX4* homologs have conserved this mitochondria-related function, we compared the mitochondrial oxygen consumption rates of the *Caenorhabditis elegans* strain *asps-1*(*ok915*), carrying a mutation in the *UBX4* homolog gene, with that of a control strain N2. Although we observed that *asps-1*(*ok915*) mutant has slow larval development (data not shown), a phenotype observed in other *C. elegans* mutants with mild mitochondrial dysfunction (43–45), we could not observe alterations in mitochondrial oxygen consumption in this mutant (Fig. S4). Although Ubx4p may not have a conserved role in mitochondrial function in *C. elegans*, we also speculate that *asps-1* can have a conditional or tissue-specific function that is not reflected by the assay performed with whole adult worms under the specific conditions used. Supporting this notion, it was recently observed that muscle-specific TUG/ASPSCR1 deletion decreases oxygen consumption and influences mitochondrial morphology only when mice are subjected to a high-fat diet (46). Although other experiments need to be performed to fully address this issue, these results suggest that Ubx4p homologs can also impact mitochondrial function in metazoans.

So, how does the deletion of *UBX4* causes dysfunction in mitochondrial metabolism? We measured the mitochondrial DNA content per cell as an indicator of the total mitochondrial content but could not observe any difference between *ubx4*Δ and control strains (Fig. S5*A*). However, we did observe a decreased respiratory capacity of mitochondria preparations from *ubx4*Δ cells when compared with preparations from control cells (Fig. S3, *B* and *C*), indicating that the mitochondria itself is functionally affected by the deletion of *UBX4*. We also reasoned that the *ubx4*Δ strain could manifest redox alterations that might explain the decrease in cell growth. We tested whether the supplementation with the antioxidant *N*-acetylcysteine would recover *ubx4*Δ growth on lithium and galactose, but no significant difference was observed (Fig. S5*B*). Recently, another protein that contains the UBX domain involved in ERAD pathway, Ubx2p, was shown to be necessary for solving defects in mitochondrial protein translocation via regulation of Cdc48p activity associated with the TOM complex (47). We tested whether the deletion of *UBX2* would mimic the phenotype observed in *ubx4*Δ of reduced growth on lithium and

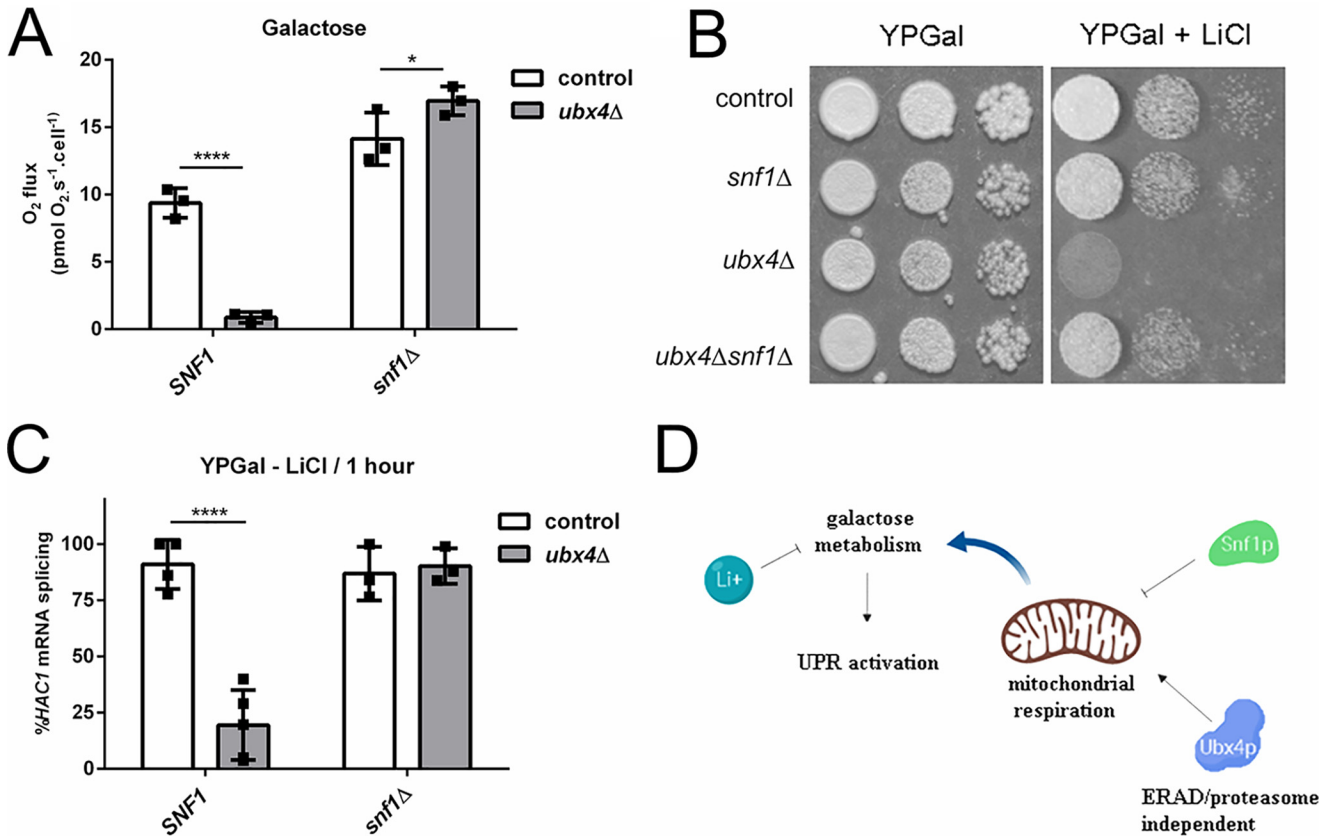

Figure 6. The deletion of *SNF1* recovers *ubx4*Δ phenotypes in lithium and galactose. *A*, the oxygen consumption rate was measured on the indicated strains grown in YPGal ($n = 3$ biological replicates). Two-way ANOVA was performed with Sidak's multiple comparisons test. *SNF1* represents strains with functional *SNF1* and *snf1*Δ represents strains harboring the deletion of the *SNF1* gene. ****, $p < 0.0001$; *, $p < 0.05$. *B*, growth test assay of the indicated strains grown in YPGal or YPGal plus 30 mM LiCl for 3 days at 30 °C. Representative results of at least three independent experiments are shown. *C*, the splicing of *HAC1* mRNA was assessed by RT-PCR from cells grown in the presence of 30 mM LiCl in YPGal for 1 h. Multiple *t* tests were performed in this case. ****, $p < 0.0001$. *D*, graphic scheme representing how Ubx4p/mitochondria axis regulates UPR activation in lithium–galactose–treated cells.

galactose, but we did not observe any significant differences on *ubx2*Δ strain growth under this condition (Fig. S2). This result suggests that Ubx2p and Ubx4p have distinct roles to sustain mitochondrial function, at least when cells are grown on galactose. Supporting this hypothesis, it was already shown that Cdc48p has distinct roles in regulating mitochondrial morphology, proteostasis, and yeast capacity to grow in medium containing respiratory carbon source (48–51). Despite our results suggesting that proteasome function may not be involved with the mitochondrial phenotypes of the *ubx4*Δ strain, it has been determined that the ubiquitin–proteasome system is involved in the control of mitochondrial function (52). We are currently trying to understand mechanistically the role of Ubx4p in the function of mitochondria, including a possible cooperation with Cdc48p.

It has been previously shown that when yeast cells are grown in the presence of galactose, inhibition of phosphoglucomutase activity by either *PGM2* gene deletion or lithium treatment results in an increase in cellular calcium uptake and UPR activation and negatively impacts cell growth (10, 53, 54). It was proposed that the increased cellular calcium accumulation is induced by an increase in the glucose-1-phosphate/glucose-6-phosphate ratio because the deletion of the *PFK2* gene (which encodes for phosphofructokinase) decreases the glucose-1-phosphate/glucose-6-phosphate ratio and concomitantly suppresses intracellular calcium accumulation (10, 55). We found that *PFK2* gene deletion did not affect UPR activation by lithium and galactose treatment (Fig. S6*A*), although it did confer some growth tolerance (Fig. S6*B*) as previously reported (10). These results suggest that the UPR activation observed under our experimental conditions is not influenced by the glucose-1-phosphate/glucose-6-phosphate ratio.

The deletion of the yeast AMPK/*SNF1* gene increases oxygen consumption in control and *ubx4*Δ cells, allowing a normal galactose metabolism and UPR activation with the treatment of lithium. Although in mammals the role of AMPK to sustain oxidative metabolism is well-characterized (56), in yeast the deletion of *SNF1* seems to increase mitochondrial respiration by enhancing amino acid uptake and utilization (42). The deletion of *SNF1* was already shown to regulate UPR activation in cells treated with tunicamycin (57). The relationship between ER stress and mitochondria was further explored by a recent study showing that mitochondrial function is necessary for cellular adaptation to DTT or tunicamycin (58). Thus, different ER stress conditions may share pathways to mediate the communication between mitochondria and the ER to allow the cell to adapt to stress.

In this work, we show interorganelle communication between mitochondria and ER through the regulation of galactose metabolism. Mitochondria during stressful conditions, such as

impaired proteostasis or energy deprivation, can send signals to the nucleus in a form of retrograde signaling to re-establish homeostasis (59). In yeast, one mechanism to mediate this communication is through the RTG pathway (60). Nevertheless, we did not observe a correlation between the decreased oxygen consumption rates and increased expression of the *CIT2* gene, a target of the RTG pathway, in the *ubx4*Δ strain (data not shown). Still, it will be interesting to test whether this signaling between mitochondria and galactose metabolism is conserved in other biological systems. In mammals, galactose metabolism is regulated by UPR after feeding (61). Thus, it is tempting to conceive that our results are a description of a primitive signaling that was modified during evolution to adapt to galactose toxicity in the context of postprandial metabolic changes. Our findings provide a link between mitochondrial homeostasis and UPR activation regulated by Ubx4p and contribute to our understanding of toxicity mediated by lithium and by galactose metabolism disturbances.

Experimental procedures

Yeast strains and growth conditions

Unless otherwise stated, all *Saccharomyces cerevisiae* strains used in this work are derived from the MATa deletion library (Open Biosystems) and have the same background of BY4741 (MATa, *his3Δ1*, *leu2Δ0*, *met15Δ0*, *ura3Δ0*). The strain *lys2*Δ was used as control strain in our assays, labeled as a control in the figures, because most strains derived from the deletion library are slightly more resistant to lithium and galactose than the parental BY4741 strain (3). Yeast cells were grown by shaking at 30 °C in YP medium (1% yeast extract, 2% Bacto peptone) containing 2% glucose (YPD), 2% galactose (YPGal), or 2% glycerol (YPGly). For plates, 2% of agar was included in the medium. Antimycin A (ethanol), *N*-acetylcysteine (water), and lithium chloride (water) were obtained from Sigma–Aldrich. The double mutant *ubx4*Δ*snf1*Δ was generated by crossing a haploid MATa *ubx4*Δ strain with a haploid MAT*α* *snf1*Δ strain previously generated by our group (62). Strains were genotyped using the following primers: SNF1A (5′-TAAGAGTATGGCACATCAACAGGTA-3′), SNF1D (5′-TGTAGTAGGTTGTATTTTTGTCGCA-3′), UBX4A (5′-TAAAACGCTAGATGCTATTTCTTGC-3′), UBX4D (5′-GAATACAATATCCCATTTGATCAGG-3′), kanB (5′-CTGCAGCGAGGAGCCGTAAT-3′), and kanC3 (5′-CCTCGACATCATCTGCCCAGAT-3′).

HAC1 transcript splicing analysis

Total RNA was extracted as previously described (3) from cells grown to the exponential phase (~0.3 $A_{600\,nm}$) under the conditions described in each experiment. A total of 1 μg of total RNA was used to prepare the first-strand cDNA using a high-capacity cDNA reverse-transcription kit following the manufacturer's protocol (Applied Biosystems, Foster City, CA). The cDNA was used as a template for the amplification of *HAC1* cDNA by PCR. The PCR conditions were 94 °C for 1 min followed by 35 cycles at 94 °C for 30 s, 62 °C for 30 s, 72 °C for 90 s, and a final step of 72 °C for 10 min. The primers used in these reactions were HAC1F (5′-GACCACGAAGACGCGTTG-3′) and HAC1R (5′-TCAAATGAATTCAAACCTGACTG-3′). The percentage of *HAC1* mRNA in the spliced form was quantified as previously described (3) using ImageJ software.

Quantitative RT-PCR

Total RNA extraction and first-strand cDNA synthesis were performed as described under "HAC1 transcript splicing analysis." Quantitative PCR was performed with the StepOnePlus real-time PCR system (Applied Biosystems) with the PCR protocol as one cycle for 10 min at 95 °C, followed by 40 cycles of 15 s at 95 °C and 45 s at 60 °C, using Power SYBR-Green PCR master mix (Applied Biosystems). The relative expression levels were calculated using the comparative Ct method (63) using *TFC1* as a reference gene (64). The sequences of the primers used in this section are TFC1F (5′-TGGATGACGTTGATGCAGAT-3′), TFC1R (5′-GCTCGCTTTTCATTGTTTCC-3′), GAL1F (5′-TTGCGAACACCCTTGTTGTA-3′), GAL1R (5′-CGTGCTCGATCCTTCTTTTC-3′), GAL2F (5′-GTCAGTTGGCCTGGATGATT-3′), and GAL2R (5′-TCCCAAGTTTTCGACAGTCC-3′). For the experiments measuring mitochondrial DNA content, we extracted the DNA as previously described (65, 66). Briefly, strains had their DNA extracted by basic phenol (pH 8.0) and chloroform (1:1) and precipitated with ethanol containing 0.3 M of sodium acetate. The primers used were COX3F (5′-TTGAAGCTGTACAACCTACC-3′), COX3R (5′-CCTGCGATTAAGGCATGATG-3′), TAF10F (5′-TTCCCAGGTATTGCCGAAA-3′), and TAF10R (5′-TTGTGGTGAACGATAGATGGA-3′).

Plate growth assay

The cells were grown overnight, and by using a replica plater for 96-well plates (Sigma R2508), serial dilutions of the cultures (prepared in sterile-distilled water to $A_{600\,nm}$ values of 0.3, 0.03, and 0.003) were transferred to plates containing the indicated medium in the figure legends. The plates were incubated at 30 °C for 3 days and then photographed. The images were processed using the Adobe Photoshop software.

Measurement of intracellular galactose and galactose-1-phosphate levels

Yeast cultures were inoculated in YPGal and maintained at 30 °C with agitation (200 rpm) until an $A_{600\,nm}$ of ~ 0.2 was reached. At this point, lithium chloride (30 mM) was added to the media, and after 1 h, the cells were collected and processed as previously described (9).

Respiration rate in vivo

The cells were grown at YPGal or YPGly until an $A_{600\,nm}$ of 0.5 was reached and then collected by centrifugation. The cells were suspended at their respective medium to achieve a concentration of 0.1 $A_{600\,nm}$, and their oxygen consumption rates were measured using the O2k oxygraph of high resolution (Oroboros) at 30 °C. After the total oxygen consumption rate was measured, antimycin A was added (final concentration used was 1 μM) to estimate the mitochondrial (antimycin A–sensitive) oxygen consumption rate.

Respiration rate in vitro

Yeast cells were grown in YPGly medium up to mid-log phase and ~100 $A_{600\,nm}$ of cells were harvested by centrifugation

(3,000 × *g*, 5 min) for mitochondria isolation as described previously (67), using 100 mg/ml of the Lallzyme MMX enzyme for cell wall digestion (Lallemand/GER) instead of Zymolyase. After isolation, mitochondria protein content was determined by the Lowry method, and the amount relative to 200 μg of proteins of the mitochondria preparation was added to the Oroboros O2k chamber containing respiration medium (0.6 M mannitol, 10 mM K_2HPO_4, 2 mM $MgCl_2$, 20 mM Hepes, pH 6.8). Glycerol-3-phosphate (30 mM), pyruvate (10 mM), malate (5 mM), and succinate (20 mM) salts were added to load the electron transport chain of isolated mitochondria, and the oxygen consumption rate was determined (nonphosphorylation state of respiration). Then the oxygen consumption rate was measured in the presence of an excess (1 mM) of ADP (phosphorylation state of respiration), and the respiratory control ratio was calculated between the two states of respiration. After the total oxygen consumption rates were measured in the two states of respiration, antimycin A was added (1 microM) to estimate the mitochondrial (antimycin A–sensitive) oxygen consumption rate. Finally, cytochrome *c* (0.5 μM) was added to inform the integrity of the membranes of the mitochondria preparation.

C. elegans experiments

Worms were grown at 20 °C as previously described (68, 69). We used the WT N2 and *asps-1*(*ok915*) V/RB994 strains. For the oxygraphy experiments, the worms were grown in *Escherichia coli* OP-50 as the food source until day 0 of adulthood at a density of ~12,000 worms/plate (90 × 15 mm). Adult worms at day 0 of adulthood were washed out from plates with MilliQ water and transferred to microtubes at a final density of 2,000–7,000 worms/biological replicate. The worms were washed two additional times with MilliQ water to remove bacteria. The water was removed, and M9 buffer was added. Oxygen consumption rate was measured at O2K oxygraph of high resolution (Oroboros) at 20 °C in M9 buffer. After oxygen consumption measurement, sodium azide was added (final concentration used was 10 mM) to estimate the organism mitochondrial oxygen consumption rate. At the end of the assay, the worms were transferred to a safe-lock tube; supernatant was removed after decantation of the worms, and the tubes were quickly frozen in liquid nitrogen. For protein extraction, 500 μl of radioimmune precipitation assay buffer was added to frozen samples and worms lysed using Bullet Blender Tissue Lyzer (two cycles of 3 min at speed 7). The samples were kept on ice for 30 min, with gentle mixing every 10 min, and centrifuged at 14,000 × *g* for 30 min at 4 °C. The supernatant containing proteins was diluted 10× and used for protein quantification by BCA protein assay kit (Pierce). Oxygen consumption rates were normalized by protein levels.

Statistical analysis

All data are presented as means ± S.D. or ± S.E. We used GraphPad Prism version 6.00 for Windows (GraphPad Software) for all analysis in this work. The specific tests and post hoc tests are indicated in the figures legends.

Author contributions—E. A. D.-S., F. S. A. P., and C. A. M. conceptualization; E. A. D.-S., F. S. A. P., and C. A. M. data curation; E. A. D.-S., F. S. A. P., and C. A. M. formal analysis; E. A. D.-S., F. S. A. P., A. L. F. V. D.-Q., H. C., M. L. F.-F., C. M. M., and S. P. investigation; E. A. D.-S., F. S. A. P., and C. A. M. writing-original draft; E. A. D.-S., F. S. A. P., A. L. F. V. D.-Q., H. C., M. L. F.-F., C. M. M., S. P., A. G., M. A. M., M. M.-L., and C. A. M. writing-review and editing; A. G., M. A. M., and M. M.-L. resources; M. A. M., M. M.-L., and C. A. M. funding acquisition; C. A. M. supervision; C. A. M. project administration.

Acknowledgments—We thank all members of the Laboratório de Bioquímica e Biologia Molecular de Leveduras for discussions and suggestions during the development of this work. We thank the members of the Obesity and Comorbidities Research Center/UNICAMP, especially Dimitrius Santiago P. S. F. Guimarães, for the technical support in the C. elegans respiration experiments. The *C. elegans strains were provided by the Caenorhabditis Genetics Center, which is funded by National Institutes of Health Office of Research Infrastructure Programs Grant P40 OD010440.*

References

1. Phiel, C. J., and Klein, P. S. (2001) Molecular targets of lithium action. *Annu. Rev. Pharmacol. Toxicol.* **41,** 789–813 CrossRef Medline
2. Masuda, C. A., Xavier, M. A., Mattos, K. A., Galina, A., and Montero-Lomeli, M. (2001) Phosphoglucomutase is an *in vivo* lithium target in yeast. *J. Biol. Chem.* **276,** 37794–37801 Medline
3. De-Souza, E. A., Pimentel, F. S., Machado, C. M., Martins, L. S., da-Silva, W. S., Montero-Lomelí, M., and Masuda, C. A. (2014) The unfolded protein response has a protective role in yeast models of classic galactosemia. *Dis. Model. Mech.* **7,** 55–61 CrossRef Medline
4. Masuda, C. A., Previato, J. O., Miranda, M. N., Assis, L. J., Penha, L. L., Mendonça-Previato, L., and Montero-Lomelí, M. (2008) Overexpression of the aldose reductase GRE3 suppresses lithium-induced galactose toxicity in *Saccharomyces cerevisiae*. *FEMS Yeast Res.* **8,** 1245–1253 CrossRef Medline
5. Nagy, T., Frank, D., Kátai, E., Yahiro, R. K., Poór, V. S., Montskó, G., Zrínyi, Z., Kovács, G. L., and Miseta, A. (2013) Lithium induces ER stress and *N*-glycan modification in galactose-grown Jurkat cells. *PLoS One* **8,** e70410 CrossRef Medline
6. Berry, G. T. (2017) in *Classic Galactosemia and Clinical Variant Galactosemia* (Adam, M., Ardinger, H., Pagon, R., Wallace, S., Bean, L., Stephens, K., Amemiya, A., eds) University of Washington, Seattle
7. Fridovich-Keil, J. L. (2006) Galactosemia: the good, the bad, and the unknown. *J. Cell. Physiol.* **209,** 701–705 CrossRef Medline
8. Botstein, D., Chervitz, S. A., and Cherry, J. M. (1997) Yeast as a model organism. *Science* **277,** 1259–1260 CrossRef Medline
9. Machado, C. M., De-Souza, E. A., De-Queiroz, A. L. F. V., Pimentel, F. S. A., Silva, G. F. S., Gomes, F. M., Montero-Lomelí, M., and Masuda, C. A. (2017) The galactose-induced decrease in phosphate levels leads to toxicity in yeast models of galactosemia. *Biochim. Biophys. Acta Mol. Basis Dis.* **1863,** 1403–1409 CrossRef Medline
10. Csutora, P., Strassz, A., Boldizsár, F., Németh, P., Sipos, K., Aiello, D. P., Bedwell, D. M., and Miseta, A. (2005) Inhibition of phosphoglucomutase activity by lithium alters cellular calcium homeostasis and signaling in *Saccharomyces cerevisiae*. *Am. J. Physiol. Cell Physiol.* **289,** C58–C67 CrossRef Medline
11. Bro, C., Regenberg, B., Lagniel, G., Labarre, J., Montero-Lomelí, M., and Nielsen, J. (2003) Transcriptional, proteomic, and metabolic responses to lithium in galactose-grown yeast cells. *J. Biol. Chem.* **278,** 32141–32149 CrossRef Medline
12. Slepak, T. I., Tang, M., Slepak, V. Z., and Lai, K. (2007) Involvement of endoplasmic reticulum stress in a novel classic galactosemia model. *Mol. Genet. Metab.* **92,** 78–87 CrossRef Medline

13. Balakrishnan, B., Chen, W., Tang, M., Huang, X., Cakici, D. D., Siddiqi, A., Berry, G., and Lai, K. (2016) Galactose-1 phosphate uridylyltransferase (GalT) gene: A novel positive regulator of the PI3K/Akt signaling pathway in mouse fibroblasts. *Biochem. Biophys. Res. Commun.* **470,** 205–212 CrossRef Medline
14. Cox, J. S., and Walter, P. (1996) A novel mechanism for regulating activity of a transcription factor that controls the unfolded protein response. *Cell* **87,** 391–404 CrossRef Medline
15. Ron, D., and Walter, P. (2007) Signal integration in the endoplasmic reticulum unfolded protein response. *Nat. Rev. Mol. Cell Biol.* **8,** 519–529 CrossRef Medline
16. Travers, K. J., Patil, C. K., Wodicka, L., Lockhart, D. J., Weissman, J. S., and Walter, P. (2000) Functional and genomic analyses reveal an essential coordination between the unfolded protein response and ER-associated degradation. *Cell* **101,** 249–258 CrossRef Medline
17. Henis-Korenblit, S., Zhang, P., Hansen, M., McCormick, M., Lee, S.-J., Cary, M., and Kenyon, C. (2010) Insulin/IGF-1 signaling mutants reprogram ER stress response regulators to promote longevity. *Proc. Natl. Acad. Sci. U.S.A.* **107,** 9730–9735 CrossRef Medline
18. Kaufman, R. J., Scheuner, D., Schröder, M., Shen, X., Lee, K., Liu, C. Y., and Arnold, S. M. (2002) The unfolded protein response in nutrient sensing and differentiation. *Nat. Rev. Mol. Cell Biol.* **3,** 411–421 CrossRef Medline
19. Urra, H., Dufey, E., Avril, T., Chevet, E., and Hetz, C. (2016) Endoplasmic reticulum stress and the hallmarks of cancer. *Trends Cancer* **2,** 252–262 CrossRef Medline
20. Scheper, W., and Hoozemans, J. J. (2015) The unfolded protein response in neurodegenerative diseases: a neuropathological perspective. *Acta Neuropathol.* **130,** 315–331 CrossRef Medline
21. Thibault, G., and Ng, D. T. W. (2012) The endoplasmic reticulum–associated degradation pathways of budding yeast. *Cold Spring Harb. Perspect. Biol.* **4,** pii: a013193 CrossRef
22. Alberts, S. M., Sonntag, C., Schäfer, A., and Wolf, D. H. (2009) Ubx4 modulates cdc48 activity and influences degradation of misfolded proteins of the endoplasmic reticulum. *J. Biol. Chem.* **284,** 16082–16089 CrossRef Medline
23. Chien, C.-Y., and Chen, R.-H. (2013) Cdc48 chaperone and adaptor Ubx4 distribute the proteasome in the nucleus for anaphase proteolysis. *J. Biol. Chem.* **288,** 37180–37191 CrossRef Medline
24. Decottignies, A., Evain, A., and Ghislain, M. (2004) Binding of Cdc48p to a ubiquitin-related UBX domain from novel yeast proteins involved in intracellular proteolysis and sporulation. *Yeast* **21,** 127–139 CrossRef Medline
25. Hartmann-Petersen, R., and Gordon, C. (2004) Integral UBL domain proteins: a family of proteasome interacting proteins. *Semin. Cell Dev. Biol.* **15,** 247–259 CrossRef Medline
26. Madsen, L., Molbæk, K., Larsen, I. B., Nielsen, S. V., Poulsen, E. G., Walmod, P. S., Hofmann, K., Seeger, M., Chien, C.-Y., Chen, R.-H., Kriegenburg, F., and Hartmann-Petersen, R. (2014) Human ASPL/TUG interacts with p97 and complements the proteasome mislocalization of a yeast ubx4 mutant, but not the ER-associated degradation defect. *BMC Cell Biol.* **15,** 31 CrossRef Medline
27. Bogan, J. S., Hendon, N., McKee, A. E., Tsao, T.-S., and Lodish, H. F. (2003) Functional cloning of TUG as a regulator of GLUT4 glucose transporter trafficking. *Nature* **425,** 727–733 CrossRef Medline
28. Bogan, J. S., Rubin, B. R., Yu, C., Löffler, M. G., Orme, C. M., Belman, J. P., McNally, L. J., Hao, M., and Cresswell, J. A. (2012) Endoproteolytic cleavage of TUG protein regulates GLUT4 glucose transporter translocation. *J. Biol. Chem.* **287,** 23932–23947 CrossRef Medline
29. Yu, C., Cresswell, J., Löffler, M. G., and Bogan, J. S. (2007) The glucose transporter 4-regulating protein TUG is essential for highly insulin-responsive glucose uptake in 3T3-L1 adipocytes. *J. Biol. Chem.* **282,** 7710–7722 CrossRef Medline
30. Hiller, M. M., Finger, A., Schweiger, M., and Wolf, D. H. (1996) ER degradation of a misfolded luminal protein by the cytosolic ubiquitin–proteasome pathway. *Science* **273,** 1725–1728 CrossRef Medline
31. Mannhaupt, G., Schnall, R., Karpov, V., Vetter, I., and Feldmann, H. (1999) Rpn4p acts as a transcription factor by binding to PACE, a nonamer box found upstream of 26S proteasomal and other genes in yeast. *FEBS Lett.* **450,** 27–34 CrossRef Medline
32. Xie, Y., and Varshavsky, A. (2001) RPN4 is a ligand, substrate, and transcriptional regulator of the 26S proteasome: a negative feedback circuit. *Proc. Natl. Acad. Sci. U.S.A.* **98,** 3056–3061 CrossRef Medline
33. Jelinsky, S. A., Estep, P., Church, G. M., and Samson, L. D. (2000) Regulatory networks revealed by transcriptional profiling of damaged *Saccharomyces cerevisiae* cells: Rpn4 links base excision repair with proteasomes. *Mol. Cell. Biol.* **20,** 8157–8167 CrossRef Medline
34. Lai, K., Boxer, M. B., and Marabotti, A. (2014) GALK inhibitors for classic galactosemia. *Future Med. Chem.* **6,** 1003–1015 CrossRef Medline
35. Hess, D. C., Myers, C. L., Huttenhower, C., Hibbs, M. A., Hayes, A. P., Paw, J., Clore, J. J., Mendoza, R. M., Luis, B. S., Nislow, C., Giaever, G., Costanzo, M., Troyanskaya, O. G., and Caudy, A. A. (2009) Computationally driven, quantitative experiments discover genes required for mitochondrial biogenesis. *PLoS Genet.* **5,** e1000407 CrossRef Medline
36. Li, Y., Chen, G., and Liu, W. (2010) Multiple metabolic signals influence GAL gene activation by modulating the interaction of Gal80p with the transcriptional activator Gal4p. *Mol. Microbiol.* **78,** 414–428 CrossRef Medline
37. Ferreira Júnior, J. R., Ramos, A. S., Chambergo, F. S., Stambuk, B. U., Muschellack, L. K., Schumacher, R., and El-Dorry, H. (2006) Functional expression of the maize mitochondrial URF13 down-regulates galactose-induced GAL1 gene expression in *Saccharomyces cerevisiae*. *Biochem. Biophys. Res. Commun.* **339,** 30–36 CrossRef Medline
38. Jelicić, B., Traven, A., Filić, V., and Sopta, M. (2005) Mitochondrial dysfunction enhances Gal4-dependent transcription. *FEMS Microbiol. Lett.* **253,** 207–213 CrossRef Medline
39. Clarke, C. F., Williams, W., and Teruya, J. H. (1991) Ubiquinone biosynthesis in *Saccharomyces cerevisiae*: isolation and sequence of COQ3, the 3,4-dihydroxy-5-hexaprenylbenzoate methyltransferase gene. *J. Biol. Chem.* **266,** 16636–16644 Medline
40. Norais, N., Prome, D., and Velours, J. (1991) ATP synthase of yeast mitochondria. Characterization of subunit d and sequence analysis of the structural gene ATP7. *J. Biol. Chem.* **266,** 16541–16549
41. Graef, M., and Nunnari, J. (2011) Mitochondria regulate autophagy by conserved signalling pathways. *EMBO J.* **30,** 2101–2114 CrossRef Medline
42. Nicastro, R., Tripodi, F., Guzzi, C., Reghellin, V., Khoomrung, S., Capusoni, C., Compagno, C., Airoldi, C., Nielsen, J., Alberghina, L., and Coccetti, P. (2015) Enhanced amino acid utilization sustains growth of cells lacking Snf1/AMPK. *Biochim. Biophys. Acta* **1853,** 1615–1625 CrossRef Medline
43. Rea, S. L., Ventura, N., and Johnson, T. E. (2007) Relationship between mitochondrial electron transport chain dysfunction, development, and life extension in *Caenorhabditis elegans*. *PLoS Biol.* **5,** e259 CrossRef Medline
44. Feng, J., Bussière, F., and Hekimi, S. (2001) Mitochondrial electron transport is a key determinant of life span in *Caenorhabditis elegans*. *Dev. Cell.* **1,** 633–644 CrossRef Medline
45. Wu, Z., Senchuk, M. M., Dues, D. J., Johnson, B. K., Cooper, J. F., Lew, L., Machiela, E., Schaar, C. E., DeJonge, H., Blackwell, T. K., and Van Raamsdonk, J. M. (2018) Mitochondrial unfolded protein response transcription factor ATFS-1 promotes longevity in a long-lived mitochondrial mutant through activation of stress response pathways. *BMC Biol.* **16,** 147 CrossRef Medline
46. Habtemichael, E. N., Li, D. T., Camporez, J. P., Westergaard, X. O., Sales, C. I., Liu, X., López-Giráldez, F., DeVries, S. G., Li, H., Ruiz, D. M., Wang, K. Y., Sayal, B. S., Hirabara, S., Vatner, D. F., Philbrick, W., *et al.* (2019) An insulin-stimulated proteolytic mechanism links energy expenditure with glucose uptake. *bioRxiv* CrossRef
47. Mårtensson, C. U., Priesnitz, C., Song, J., Ellenrieder, L., Doan, K. N., Boos, F., Floerchinger, A., Zufall, N., Oeljeklaus, S., Warscheid, B., and Becker, T. (2019) Mitochondrial protein translocation-associated degradation. *Nature* **569,** 679–683 CrossRef Medline
48. Simões, T., Schuster, R., den Brave, F., and Escobar-Henriques, M. (2018) Cdc48 regulates a deubiquitylase cascade critical for mitochondrial fusion. *Elife* **7,** e30015 CrossRef Medline
49. Zurita Rendón, O., Fredrickson, E. K., Howard, C. J., Van Vranken, J., Fogarty, S., Tolley, N. D., Kalia, R., Osuna, B. A., Shen, P. S., Hill, C. P., Frost, A., and

Rutter, J. (2018) Vms1p is a release factor for the ribosome-associated quality control complex. *Nat. Commun.* **9,** 2197 CrossRef Medline
50. Izawa, T., Park, S.-H., Zhao, L., Hartl, F. U., and Neupert, W. (2017) Cytosolic protein Vms1 links ribosome quality control to mitochondrial and cellular homeostasis. *Cell* **171,** 890–903.e18 CrossRef Medline
51. Braun, R. J., Zischka, H., Madeo, F., Eisenberg, T., Wissing, S., Büttner, S., Engelhardt, S. M., Büringer, D., and Ueffing, M. (2006) Crucial mitochondrial impairment upon CDC48 mutation in apoptotic yeast. *J. Biol. Chem.* **281,** 25757–25767 CrossRef Medline
52. Bragoszewski, P., Turek, M., and Chacinska, A. (2017) Control of mitochondrial biogenesis and function by the ubiquitin: proteasome system. *Open Biol.* **7,** 170007 CrossRef Medline
53. Fu, L., Miseta, A., Hunton, D., Marchase, R. B., and Bedwell, D. M. (2000) Loss of the major isoform of phosphoglucomutase results in altered calcium homeostasis in *Saccharomyces cerevisiae*. *J. Biol. Chem.* **275,** 5431–5440 CrossRef Medline
54. Aiello, D. P., Fu, L., Miseta, A., Sipos, K., and Bedwell, D. M. (2004) The Ca^{2+} homeostasis defects in a pgm2Delta strain of *Saccharomyces cerevisiae* are caused by excessive vacuolar Ca^{2+} uptake mediated by the Ca^{2+}-ATPase Pmc1p. *J. Biol. Chem.* **279,** 38495–38502 CrossRef Medline
55. Aiello, D. P., Fu, L., Miseta, A., and Bedwell, D. M. (2002) Intracellular glucose 1-phosphate and glucose 6-phosphate levels modulate Ca^{2+} homeostasis in *Saccharomyces cerevisiae*. *J. Biol. Chem.* **277,** 45751–45758 CrossRef Medline
56. Herzig, S., and Shaw, R. J. (2018) AMPK: guardian of metabolism and mitochondrial homeostasis. *Nat. Rev. Mol. Cell Biol.* **19,** 121–135 CrossRef Medline
57. Mizuno, T., Masuda, Y., and Irie, K. (2015) The *Saccharomyces cerevisiae* AMPK, Snf1, negatively regulates the Hog1 MAPK pathway in ER stress response. *PLoS Genet.* **11,** e1005491 CrossRef Medline
58. Knupp, J., Arvan, P., and Chang, A. (2019) Increased mitochondrial respiration promotes survival from endoplasmic reticulum stress. *Cell Death Differ.* **26,** 487–501 CrossRef Medline
59. Haynes, C. M., Fiorese, C. J., and Lin, Y.-F. (2013) Evaluating and responding to mitochondrial dysfunction: the mitochondrial unfolded-protein response and beyond. *Trends Cell Biol.* **23,** 311–318 CrossRef Medline
60. Butow, R. A., and Avadhani, N. G. (2004) Mitochondrial signaling: the retrograde response. *Mol. Cell.* **14,** 1–15 CrossRef Medline
61. Deng, Y., Wang, Z. V., Tao, C., Gao, N., Holland, W. L., Ferdous, A., Repa, J. J., Liang, G., Ye, J., Lehrman, M. A., Hill, J. A., Horton, J. D., and Scherer, P. E. (2013) The Xbp1s/GalE axis links ER stress to postprandial hepatic metabolism. *J. Clin. Invest.* **123,** 455–468 CrossRef Medline
62. Bozaquel-Morais, B. L., Madeira, J. B., Venâncio, T. M., Pacheco-Rosa, T., Masuda, C. A., and Montero-Lomeli, M. (2017) A chemogenomic screen reveals novel Snf1p/AMPK independent regulators of acetyl-CoA carboxylase. *PLoS One* **12,** e0169682 CrossRef Medline
63. Livak, K. J., and Schmittgen, T. D. (2001) Analysis of relative gene expression data using real-time quantitative PCR and the $2(-\Delta\Delta C(T))$ method. *Methods* **25,** 402–408 CrossRef Medline
64. Teste, M.-A., Duquenne, M., François, J. M., and Parrou, J.-L. (2009) Validation of reference genes for quantitative expression analysis by real-time RT-PCR in *Saccharomyces cerevisiae*. *BMC Mol. Biol.* **10,** 99 CrossRef Medline
65. Osman, C., Noriega, T. R., Okreglak, V., Fung, J. C., and Walter, P. (2015) Integrity of the yeast mitochondrial genome, but not its distribution and inheritance, relies on mitochondrial fission and fusion. *Proc. Natl. Acad. Sci. U.S.A.* **112,** E947–E956 CrossRef Medline
66. Hoffman, C. S., and Winston, F. (1987) A ten-minute DNA preparation from yeast efficiently releases autonomous plasmids for transformation of *Escherichia coli*. *Gene* **57,** 267–272 CrossRef Medline
67. Torelli, N. Q., Ferreira-Júnior, J. R., Kowaltowski, A. J., and da Cunha, F. M. (2015) RTG1- and RTG2-dependent retrograde signaling controls mitochondrial activity and stress resistance in *Saccharomyces cerevisiae*. *Free Radic. Biol. Med.* **81,** 30–37 CrossRef Medline
68. Brenner, S. (1974) The genetics of *Caenorhabditis elegans*. *Genetics* **77,** 71–94 Medline
69. Pinto, S., Sato, V. N., De-Souza, E. A., Ferraz, R. C., Camara, H., Pinca, A. P. F., Mazzotti, D. R., Lovci, M. T., Tonon, G., Lopes-Ramos, C. M., Parmigiani, R. B., Wurtele, M., Massirer, K. B., and Mori, M. A. (2018) Enoxacin extends lifespan of C. elegans by inhibiting miR-34–5p and promoting mitohormesis. *Redox Biol.* **18,** 84–92 CrossRef Medline